

Brain networks' functional connectivity separates aphasic deficits in stroke

Antonello Baldassarre, PhD, Nicholas V. Metcalf, BA, Gordon L. Shulman, PhD, and Maurizio Corbetta, MD

Neurology® 2019;92:e125-e135. doi:10.1212/WNL.0000000000006738

Correspondence

Dr. Baldassarre
antonello.baldassarre@
gmail.com

Abstract

Objective

To investigate whether different language deficits are distinguished by the relative strengths of their association with the functional connectivity (FC) at rest of the language network (LN) and cingulo-opercular network (CON) after aphasic stroke.

Methods

In a group of patients with acute stroke and left-hemisphere damage, we identified 3 distinct, yet correlated, clusters of deficits including comprehension/lexical semantic, grapheme-phoneme knowledge, and verbal executive functions. We computed partial correlations in which the contributions of a behavioral cluster and network FC of no interest were statistically regressed out.

Results

We observed a double dissociation such that impairment of grapheme-phoneme knowledge was more associated with lower FC of the LN within the left hemisphere than lower FC of the CON, whereas verbal executive deficits were more related to lower FC of the CON than the LN in the left hemisphere. Furthermore, the specific association between language deficits and FC was independent of the amount of structural damage to the LN and CON.

Conclusion

These findings indicate that after a left-hemisphere lesion, the type of language impairment is related to the abnormal pattern of correlated activity in different networks. Accordingly, they extend the concept of a neuropsychological double dissociation from structural damage to functional network abnormalities. Finally, current results strongly argue in favor of the behavioral specificity of intrinsic brain activity after focal structural damage.

From IRCCS NEUROMED (A.B.), Pozzilli, IS, Italy; Departments of Neurology (N.V.M., G.L.S., M.C.), Radiology (M.C.), Anatomy & Neurobiology (M.C.), and Bioengineering (M.C.), Washington University in St. Louis School of Medicine, MO; Department of Neuroscience (M.C.), University of Padua; and Padua Neuroscience Center (M.C.), Italy.

Go to [Neurology.org/N](https://www.neurology.org/N) for full disclosures. Funding information and disclosures deemed relevant by the authors, if any, are provided at the end of the article.

Glossary

COMP/LEX-SEM = comprehension/lexical semantic; **CON** = cingulo-opercular network; **FC** = functional connectivity; **FDR** = false discovery rate; **FLAIR** = fluid-attenuated inversion recovery; **GRA-PHO** = grapheme-phoneme; **LN** = language network; **ROI** = region of interest; **TE** = echo time; **TR** = repetition time; **vEXE** = verbal executive.

Behavioral and lesion-mapping studies in aphasics have identified distinct profiles of language impairments, including deficits in phonological processing and semantic^{1,2} and executive-cognitive functions.^{2,3} These profiles might be associated with distinct brain regions. Anatomical-clinical correlational studies have linked damage of specific brain regions and white matter structure to distinct language impairments.^{2,4} However, numerous neuroimaging reports have shown in aphasic patients poststroke changes of activity in structurally intact brain areas distant from the site of the lesion.⁵⁻⁷

Regions in the left posterior superior temporal and left inferior frontal gyrus are important for phonological features during speaking as observed in lesion-mapping^{2,8} as well as fMRI^{9,10} studies in healthy individuals. However, verbal executive functions, e.g., verbal fluency, might recruit, besides frontal and temporal cortices,¹¹ bilateral inferior frontal gyrus/insula, thalamus, and the dorsal anterior cingulate,¹² areas of the so-called cingulo-opercular network (CON) involved in the maintenance of task-sets¹³ and/or alertness and arousal¹⁴ in multiple tasks.

Previously, we showed that a general language deficit correlated with reduced resting-state functional connectivity (FC)¹⁵ in the auditory network,¹⁶ yet, associations between different impairments and abnormalities in distinct networks were not reported. Here, we observed that the severity of phonological (specifically grapheme-phoneme knowledge) and severity of verbal executive deficits in aphasia correlated with alterations of FC of the LN and CON, respectively. These findings indicate that changes in brain networks account for distinct language impairments after stroke.

Methods

Standard protocol approvals, registrations, and patient consents

The institutional review board of Washington University in St. Louis approved the study. All participants provided informed consent.

Study design

We used the partial correlation technique to identify the (relatively) unique association between distinct language impairments and resting-state FC of different networks in a group of acute stroke patients with aphasic deficits.

Stroke patients

We first recruited a sample of 60 patients (33 women, mean age at stroke: 34.5 years, SD = 12.2; range 19–79 years) exhibiting a first-ever left-hemisphere stroke at the acute stage

(i.e., 2 weeks) from the stroke service at Barnes-Jewish Hospital. As described in Ref. 17, patients were not recruited based on specific impairments but prospectively included based on the presence of any behavioral deficit after a first time stroke. The following were inclusion criteria: (1) clinical diagnosis of left-hemisphere stroke (ischemic or hemorrhagic) at hospital discharge; (2) persistent stroke symptom(s) at hospital discharge; (3) awake, alert, and able to complete study tasks; and (4) age older than 18 years. Exclusion criteria included: (1) previous stroke; (2) multifocal stroke; (3) severe psychiatric disorders/conditions; (4) dementia (as measured by a Short Blessed Test score of ≥ 9 , or as measured by a premorbid AD8 score of ≥ 2); (5) epilepsy, Parkinson disease, or other neurologic disorder; (6) brain injury; (7) end-stage renal disease, terminal cancer, class III or IV heart failure, or other diagnosis with a life expectancy less than 1 year; (8) premorbid functional disability measured by a mean of the modified Rankin Scale score of ≥ 2 ; (9) claustrophobia; and (10) body metal not allowing 3T MRI.

After the behavioral evaluation, a final group of 33 patients who exhibited a pathologic score in at least one language test (i.e., 2 SDs below the average of healthy controls matched for age and education) was included in the study. Table 1 displays the demographic and lesion information, as well as NIH Stroke Scale scores at admission to the hospital.

Healthy controls

We also recruited a group of 34 healthy controls including individuals without any neurologic or severe psychiatric history (mean age = 55.7 years, SD = 11.5, range 21–83 years), matched for age and education with the stroke sample. All healthy controls gave written informed consent in line with the Declaration of Helsinki.

Behavioral testing of language

The neuropsychological assessment of language, fully described in our previous work,¹⁷ included the following tests: Basic Word Discrimination; Commands; Complex Ideational Material; Oral Reading of Sentences; Comprehension of Oral Reading of Sentences; Boston Naming Test short form; Nonword Reading; Stem Completion; and Category (Animal) Fluency.

Analysis of behavioral scores

To identify (relatively) distinct profiles of language deficits, the scores of the 9 behavioral tests underwent a 3-step analysis. Step 1: We computed the pairwise correlations between the normalized *z* scores of each test across the patients (*n* = 33). Step 2: We conducted a clustering analysis, implemented in MATLAB (The MathWorks Inc., Natick, MA), on the

Table 1 Demographic and clinical characteristics of the patients with left-hemisphere damage (n = 33)

ID	Age at stroke, y	Sex	tPA	Lesion type	Lesion volume, mm ³	Lesion site	Acute NIHSS score (range: 0–42; 0 = normal)
1	43	M	N	I	7,574	C-S	20
2	50	F	N	I	776	C	2
3	56	M	N	I	910	C	6
5	56	M	N	I	6,832	C-S	18
6	63	F	N	I	4,161	C	12
9	69	F	N	I	303	BS	10
12	56	M	N	I	371	BS	7
13	64	F	N	I	7,738	C	15
16	57	M	N	H	9,760	C-S	12
21	72	M	N	I	584	C	1
24	28	M	N	I	10,110	C-S	21
26	54	M	Y	I	13,895	C-S	13
27	42	F	N	I	5,160	C-S	2
28	58	F	N	I	2,007	CBL	3
29	38	M	N	I	162	S	4
30	53	F	N	H	11,301	C-S	21
34	70	M	N	I	6,287	C	4
35	64	F	N	I	1,224	S	11
36	58	F	N	I	7,104	C	6
37	79	M	N	H	8,188	C-S	11
38	61	M	N	I	3,911	C	NA
40	64	F	Y	I	6,975	C	8
42	54	F	N	H	34,627	C-S	18
43	59	M	Y	I	5,369	C-S	15
46	43	M	N	I	2,714	C	13
47	58	M	N	I	6,103	C-S	12
48	50	F	N	I	1,451	WM	17
49	62	M	N	H	3,262	S	12
50	45	M	N	I	1,222	C	0
52	65	F	N	I	596	S	4
53	40	M	N	H	5,116	S	10
54	50	M	N	I	3,332	C-S	4
58	59	F	N	I	13,627	C-S	NA
Total	—	19 M, 14 F	3 Y, 30 N	27 I, 6 H	—	15 C, 5 S, 13 C-S, 1 CBL, 1 WM, 2 BS	
Mean	55.9	—	—	—	5,841	—	10.1
SD	10.8	—	—	—	6,468	—	6.2

Abbreviations: BS = brainstem; C = cortical; CBL = cerebellum; C-S = cortico-subcortical; H = hemorrhagic; I = ischemic; N = no; NA = not available; NIHSS = NIH Stroke Scale; S = subcortical; tPA = tissue plasminogen activator; WM = white matter; Y = yes.

correlation matrix to isolate clusters of tests. We first computed the “cityblock” distance between pairs of objects (i.e., correlation among tests) and then created a hierarchical cluster tree based on the unweighted average distance of the data points. The goodness of different cluster solutions, e.g., grouping in *n*-clusters, was assessed with a “clustering fitness” index, which was obtained by multiplying the Dunn and Silhouette indices. The former indicates the quotient between the shortest distance between elements of distinct clusters and the maximum distance between points belonging to the same cluster; the latter denotes how a given point is similar to the other points belonging to the same cluster, in relation to points in different clusters. Step 3: For each patient, we averaged the scores of the tests falling in the same cluster to obtain a single cluster score.

fMRI procedure

MRI scanning was performed with a Siemens 3T TIM-TRIO scanner (Siemens Medical Solutions, Malvern, PA) at the Washington University School of Medicine and conducted as in our previous studies.^{18–20} Structural scans consisted of the following: (1) a sagittal T1-weighted magnetization-prepared rapid-acquisition gradient echo (repetition time [TR] = 1,950 milliseconds [ms], echo time [TE] = 226 ms, flip angle = 9°, voxel size = 1.0 × 1.0 × 1.0 mm); (2) a transverse T2-weighted turbo spin-echo (TR = 2,500 ms, TE = 442 ms, voxel size = 1.0 × 1.0 × 1.0 mm); and (3) sagittal FLAIR (fluid-attenuated inversion recovery) (TR = 7,500 ms, TE = 326 ms, voxel size = 1.5 × 1.5 × 1.5 mm). Resting-state functional scans were acquired with a gradient echo-planar imaging sequence with TR = 2,000 ms, TE = 27 ms, 32 contiguous 4-mm slices, 4 × 4 in-plane resolution, during which participants were instructed to fixate on a small white cross displayed on a black background in a low-luminance environment. Seven resting-state fMRI runs, each including 128 volumes, were acquired. Each run lasted 4.26 minutes.

fMRI data preprocessing

Functional MRI data underwent preprocessing as previously described in our study.²¹ Furthermore, in preparation for the FC MRI analysis, data were passed through several additional preprocessing steps²²: (1) spatial smoothing consisting of 6-mm full width at half maximum gaussian blur in each direction; (2) temporal filtering retaining frequencies below 0.1 Hz; and (3) removal of the following sources of spurious variance unlikely to reflect spatially specific functional correlations through linear regression: (i) 6 parameters obtained by rigid body correction of head motion, (ii) the whole-brain signal averaged over a fixed region in atlas space, (iii) signal from a ventricular region of interest (ROI), and (iv) signal from a region centered in the white matter.

Quality control of resting-state fMRI data

Before performing FC computations, we identified and removed the magnetic resonance frames contaminated by head motion through the DVARS measure (root mean square change of the temporally differentiated fMRI data averaged over the brain).²³ We defined the DVARS criterion for high

motion frames as 2 SDs above the mean DVARS in the healthy controls, corresponding to 0.46 root mean square fMRI signal change in units of percent. We then applied such frame-censoring criterion to all resting-state fMRI data of both patients and healthy controls, prior to FC analyses. Furthermore, since the delay in the hemodynamic response can affect FC measurements in stroke populations,²⁴ we calculated the lag scores in each patient for each network and we regressed out such values from any FC-behavior correlation in order to mitigate the effect of BOLD (blood oxygen level–dependent) signal delay on the FC-behavior computation. We applied on the current dataset a procedure for computing lag score, which is fully described in detail in our previous study.²⁴ For each patient and for each network (e.g., left LN), we calculated the lag value for each node (e.g., left inferior frontal gyrus). Then, we obtained the network lag value by averaging the values of the single nodes. This average value was entered in the partial correlation computation as a variable of no interest.

Lesion segmentation

As in our previous studies,^{18–20} the lesions were manually segmented using the Analyze biomedical imaging software (mayo.edu) system by inspection of the T1-weighted, T2-weighted, and FLAIR structural images, simultaneously displayed in atlas space. All segmentations were reviewed by 2 neurologists (M.C. and Alex Carter, MD). Figure 1A displays a voxelwise map of the lesion distribution, whereas table 1 reports the information regarding lesion volume (mean = 5,841 mm³; SD = 5,468).

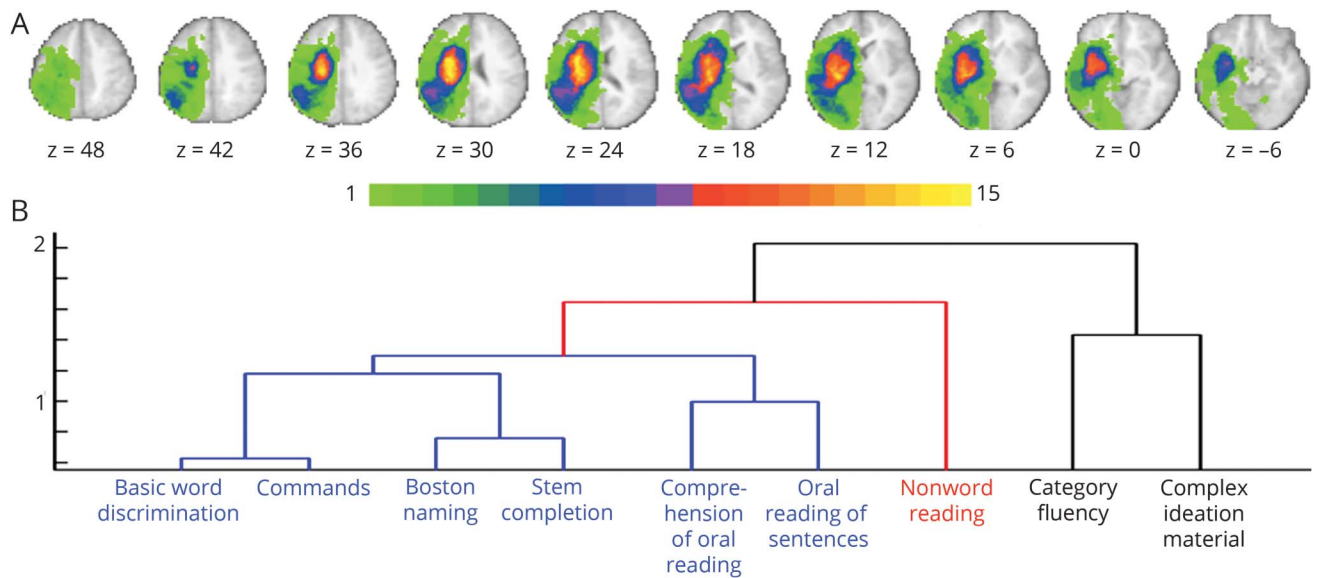
Language and cingulo-opercular networks

In the current study, we used the language network (LN) and CON (see figure 2 and table 2 for the list of ROIs) derived in an independent cohort of 21 young healthy participants (14 women, mean age 24.6 years, 23–35 years) described in our previous study.²⁵ Since the LN is known to be left-hemisphere lateralized, we focused within the left hemisphere. By contrast, because the CON is bilateral, we considered the whole network.

Correlation between language impairments and FC

We used a procedure, fully described in our previous study¹⁹ and displayed in figure 3, to obtain an FC score indexing the FC of the LN within the left hemisphere (left LN FC) and an FC score capturing the FC of the whole CON (CON FC). In the first step (figure 3A), for each patient and for each ROI, we calculated a voxelwise FC map by computing the Pearson correlation coefficient *r* between the ROI time course and the time courses from all other brain voxels. The correlation coefficients were transformed into Fisher *z* scores before any other analyses, hence generating *z*(*r*) maps. Overall, the procedure yielded 13 FC maps for each patient. Figure 3A displays one FC map obtained from ROI 1 (left inferior frontal gyrus) of the left LN in a representative patient. Albeit each map was derived from a seed region in one hemisphere, the voxelwise map itself showed the FC of that region with the whole brain. Of note, ROIs that included any lesioned voxels

Figure 1 Lesion topography and clustering of behavioral tests

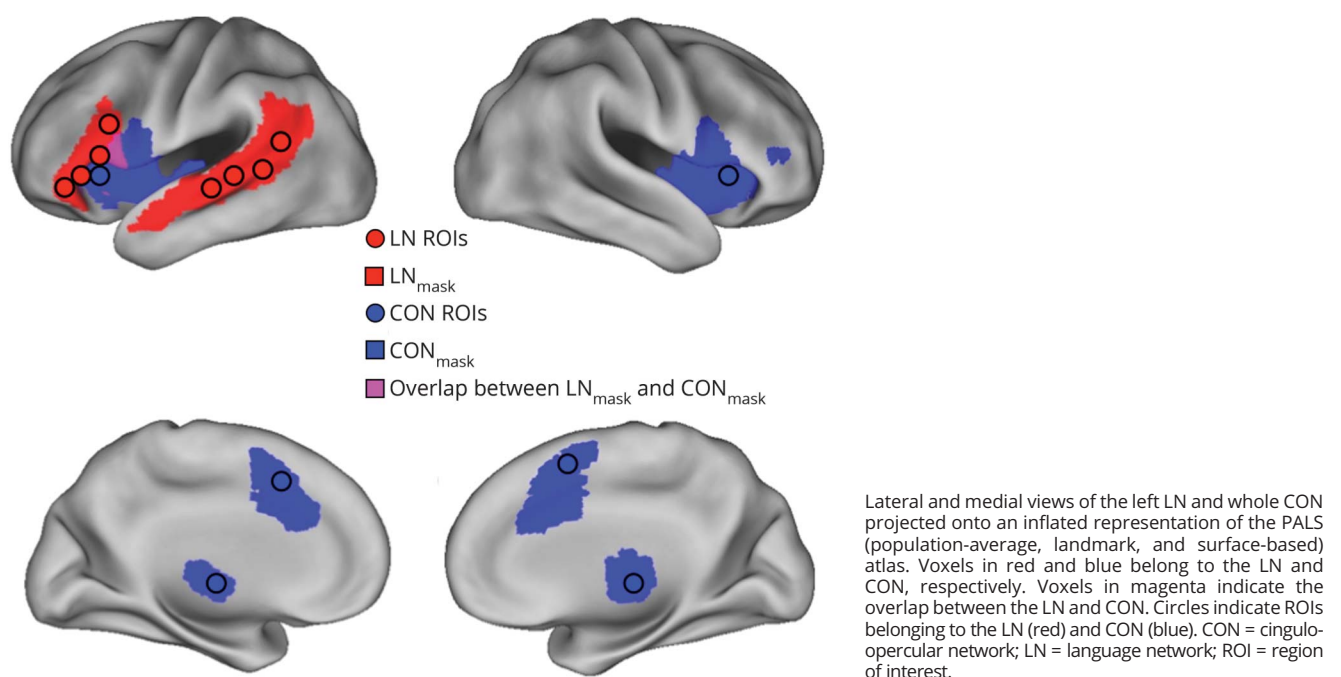


(A) Lesion density in the sample of patients ($n = 33$) for left-hemisphere lesions. The color bar indicates the number of patients with a lesion in a given voxel. (B) Dendrogram derived from applying a clustering algorithm to the correlation matrix for the behavioral tests. Blue, red, and black colors indicate tests failing in the comprehension/lexical semantic, grapheme-phoneme knowledge, and verbal executive clusters, respectively.

were not used in the analyses. Furthermore, voxels in the FC map included within the segmented lesion were not used in the FC computation of that patient's contribution to the group-level analysis. Hence, the FC maps did not contain FC values involving any damaged voxels. In the second step (figure 3, B and C), for each patient, we applied to each ROI-

based FC map a mask (derived from the dataset of young healthy individuals) of the corresponding network either in the same hemisphere (e.g., left LN_{mask}) (figure 3B) or in the opposite hemisphere (e.g., right LN_{mask}) (not shown). Therefore, for a given ROI in the left hemisphere (e.g., left inferior frontal gyrus), we obtained 2 FC masked maps, the

Figure 2 Language and cingulo-opercular networks



Lateral and medial views of the left LN and whole CON projected onto an inflated representation of the PALS (population-average, landmark, and surface-based) atlas. Voxels in red and blue belong to the LN and CON, respectively. Voxels in magenta indicate the overlap between the LN and CON. Circles indicate ROIs belonging to the LN (red) and CON (blue). CON = cingulo-opercular network; LN = language network; ROI = region of interest.

Table 2 List of regions of interest

RSN	Hemisphere	Region	X	Y	Z
LN	L	IFG	-48	30	-2
LN	L	IFG	-44	25	-2
LN	L	IFG	-50	19	9
LN	L	MFG	-45	14	21
LN	L	STG	-54	-23	-3
LN	L	STG	-56	-33	3
LN	L	STG	-48	-44	3
LN	L	STG	-52	-54	12
CON	M	dACC/msFC	-1	10	46
CON	L	aTha	-12	-15	7
CON	L	al	-33	13	9
CON	R	aTha	10	-15	8
CON	R	al	36	16	4

Abbreviations: al = anterior insula; Talairach space; aTha = anterior thalamus; CON = cingulo-opercular network; dACC/msFC = dorsal anterior cingulate cortex/middle superior frontal cortex; IFG = inferior frontal gyrus; L = left; LN = language network; M = medial; MFG = middle frontal gyrus; R = right; RSN = resting-state network; STG = superior temporal gyrus. Table lists all 13 regions of interest sorted by RSNs.

former retaining the voxels exhibiting FC between the ROI and the left LN (figure 3C), the latter including voxels showing the interhemispheric FC with the right LN (not shown). Similarly, for an ROI in the right hemisphere, we obtained a map indicating the voxels in the same hemisphere (right) and one map in the opposite hemisphere (left). This computation yielded for each ROI 4 masked FC maps: left ROI/left mask, left ROI/right mask, right ROI/left mask, and right ROI/right mask. Then, for each masked FC map, we averaged the $z(r)$ values of the voxels comprised within the borders of the network map obtaining an ROI-to-network FC score. To compute the left-hemisphere LN FC (left LN FC), we calculated the ROI-to-network scores of the maps seeded in the left hemisphere and masked with a left-hemisphere mask (figure 3, D and H). The final left LN FC score was obtained for each patient by averaging all the ROI-to-network FC scores (figure 3I). The same computation was applied to the left and right ROIs of the CON, yielding a left and right intrahemispheric FC score for each network. We then computed the interhemispheric FC score by averaging the $z(r)$ values of the voxels in the right hemisphere derived from the left ROI-based FC masked maps and the values of the voxels in the left hemisphere derived from the right ROI-based FC masked maps. The final FC score for CON was obtained by averaging the FC values of the left and right intrahemispheric FC as well as the interhemispheric FC.

To summarize, the left LN FC score indexes the FC between the left ROIs and the left voxels of the LN, while the CON FC

score captures the FC within the whole network, including the FC between an ROI and voxels in both the same and opposite hemispheres of the CON.

We then correlated in the group of patients each summary FC score with the score of the single clusters of language deficits, obtaining a “total” correlation coefficient. The factorial combination of 2 clusters of language deficits (see results section) and 2 FC summary scores yielded 4 FC-behavior total correlation scores. The total FC-behavior correlations were computed to investigate the patterns of FC associated with language impairments exclusively at a qualitative level.

Since scores for different language clusters were correlated and FC scores for different networks were correlated, we computed the partial correlation coefficients between the FC of a given network and a language deficit, statistically removing the contribution of the other behavior and the FC derived from the other network. This procedure allowed us to determine the unique association between a given cluster and network. Furthermore, to mitigate the effects of delays of the hemodynamic response due to a stroke, we regressed out the network-based lag score of each single patient from the computation of the FC-behavior partial correlation coefficients. Successively, we statistically compared the partial correlation coefficients using the Steiger z -transform test,²⁶ implemented on the web version of the software “cocorr” of the R package (comparingcorrelations.org/).²⁷ Specifically, in each comparison, we considered the 2 partial correlations as overlapping (e.g., A–B vs A–C) and based on 2 dependent groups (e.g., same group). Alpha and confidence levels were set to equal 0.05 and 0.95, respectively. We conducted a 2-tailed test of the null hypothesis A–B is equal to A–C. Finally, we used the Benjamini and Hochberg²⁸ false discovery rate (FDR) approach to correct the comparisons of the partial correlations.

Data availability

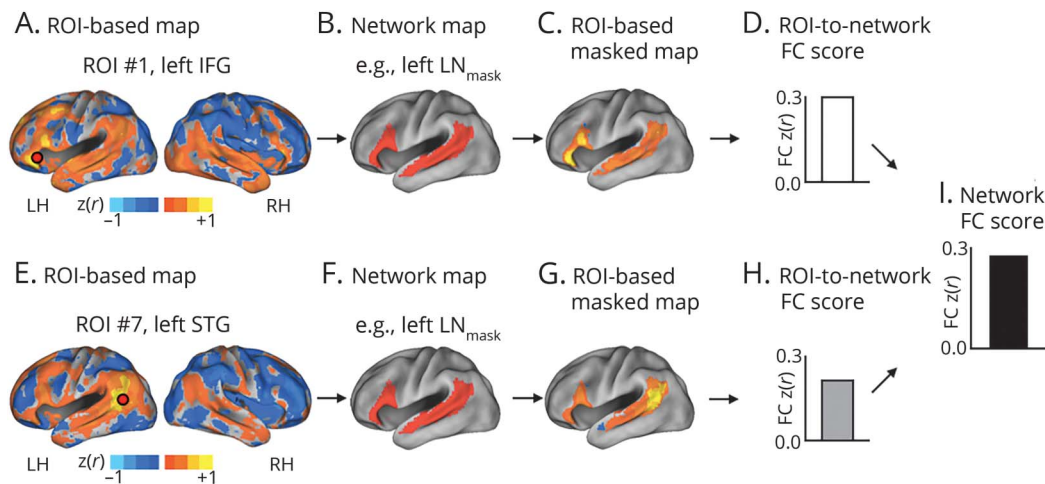
The dataset used in this analysis is available to other researchers on request to the corresponding author.

Results

Behavior

The clustering analysis on the final cohort of patients ($n = 33$) yielded 3 clusters, displayed in figure 1B. Cluster 1 comprised the majority of tests (6 of 9) evaluating comprehension (Basic Word Discrimination, Commands, Comprehension of Oral Reading of Sentences), production (Boston Naming, Stem Completion), and reading (Oral Reading of Sentences) (blue lines in figure 1B). These tests assess comprehension as well as lexical semantic functions. Accordingly, cluster 1 was labeled as “comprehension/lexical semantic” (COMP/LEX-SEM) deficit. Cluster 2 included only Nonword Reading, a test of phonological processing involving grapheme-phoneme knowledge, and therefore was labeled as “grapheme-phoneme” (GRA-PHO) deficit cluster (red line in figure

Figure 3 Flowchart of steps involved in computing FC scores



The pipeline for computing the FC score within the left LN in a single patient using real data; the full procedure is described in detail in our previous study.¹⁹ In the first step (A and E), for each patient, we computed an ROI-based (e.g., left IFG) voxelwise FC map for each ROI of each network. These maps were generated by computing the Pearson correlation coefficient r between the ROI time course and the time courses from all other brain voxels. The correlation coefficients were Fisher z -transformed prior to further analyses, thereby generating $z(r)$ maps. Orange-yellow colors indicate voxels with positive FC with the ROI; blue-cyan colors indicate negative FC. In step 2 (B–C and F–G), for each patient, we applied to each ROI-based FC map a mask (derived from the young controls and retaining voxels with $z(r) > 0.3$) of the corresponding network either to the same hemisphere (e.g., left LN_{mask}) or in the opposite hemisphere (not shown). Therefore, for a given ROI in the left hemisphere (e.g., left IFG), we obtained 2 FC masked maps, the former retaining the voxels exhibiting FC between the ROI and the left LN (C and G), the latter including voxels showing the interhemispheric FC with the right LN (not shown). Similarly, for an ROI in the right hemisphere, we obtained a map indicating the voxels in the same hemisphere (right) and one map in the opposite hemisphere (left). These computations yielded for each ROI 4 masked FC maps: left ROI/left mask, left ROI/right mask, right ROI/left mask, and right ROI/right mask. Then, for each masked FC map, we averaged the $z(r)$ values of the voxels comprised within the borders of the network map obtaining an ROI-to-network FC score (D and H). To compute the left-hemisphere LN FC (left LN FC), we calculated the ROI-to-network scores of the maps seeded in the left hemisphere and masked with left-hemisphere mask (D and H). The final left LN FC score was obtained for each patient by averaging all the ROI-to-network FC scores (I). The same computation was applied on the left and right ROIs of the cingulo-opercular (not shown), yielding a left and right intrahemispheric FC score for each network. We then computed the interhemispheric FC score by averaging the $z(r)$ values of the voxels in the right hemisphere derived from the left ROI-based FC masked maps and the values of the voxels in the left hemisphere derived from the right ROI-based FC masked maps. The final FC score for the cingulo-opercular network was obtained by averaging the FC values of the left and right intrahemispheric FC as well as the interhemispheric FC. FC = functional connectivity; IFG = inferior frontal gyrus; LH = left hemisphere; LN = language network; RH = right hemisphere; ROI = region of interest; STG = superior temporal gyrus.

1B). Finally, cluster 3 encompassed 2 different tests, Category (Animal) Fluency and Complex Ideational Material. Category Fluency involves several executive operations²⁹ such as attention, monitoring of working memory, and suppression of irrelevant information. Patients have to continuously retrieve/select words from their lexicon that match the indicated rule over a long time period (1 minute). Similarly, Complex Ideational Material recruits attention, short-term memory, and abstract reasoning.³⁰ While patients are initially required to give yes/no answers to simple questions, the complexity increases as the test proceeds. Therefore, cluster 3 was labeled as “verbal executive” (vEXE) deficit cluster (black lines in figure 1B). For each patient, we averaged the scores of the single tests within each cluster, obtaining a score for the patient’s COMP/LEX-SEM, GRA-PHO, and vEXE deficit. The same procedure was applied to the group of healthy age-matched controls.

GRA-PHO and vEXE clusters exhibited a moderate although significant degree of correlation ($p = 0.03$), whereas both clusters were strongly correlated with COMP/LEX-SEM ($p < 0.000005$), which strongly recapitulates the language factor (6 of 9 tests) associated with the FC of the auditory network in our previous study on the entire (i.e., not selected) cohort of patients.¹⁶ In light of these patterns of correlations, here, we

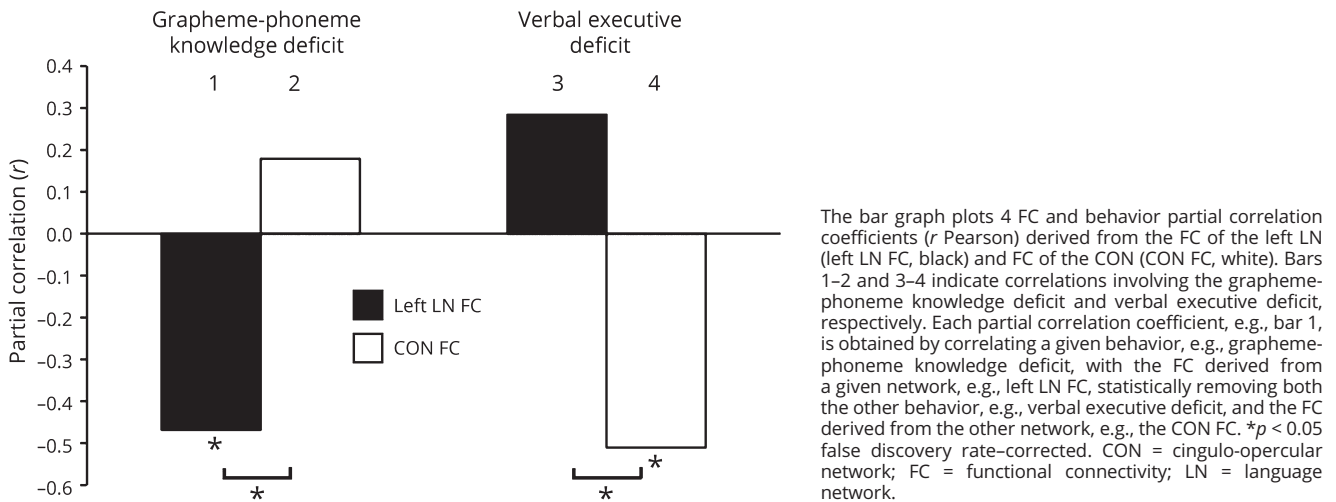
focused on the FC-behavior dissociation involving the GRA-PHO and vEXE clusters to investigate whether different language deficits were selectively associated with distinct patterns of FC.

Double dissociation between grapheme-phoneme/executive deficits and LN and CON

Given the relatively low correlation between deficits of knowledge of grapheme-phoneme rules and verbal executive functions, we investigated whether these impairments were associated with different patterns of resting-state FC of the LN and CON (see figure 2 and table 2 for the list of ROIs). Specifically, we tested the double dissociation such that the deficit of GRA-PHO was more associated with the FC of the LN than CON, while the vEXE deficit was more associated with the FC of the CON than LN.

Figure 4 displays the partial correlations of the GRA-PHO deficit and vEXE deficit with the FC of the left LN (left LN FC) and the FC of the CON (CON FC). We observed 2 significant FC-behavior partial correlations linking the deficit of grapheme-phoneme knowledge to left LN FC (bar 1, $r = -0.47$, $p = 0.009$) and the verbal executive deficit to CON FC (bar 4, $r = -0.51$, $p = 0.004$). These results indicate that patients with lower FC in the LN within the left hemisphere

Figure 4 Partial correlations between behavioral deficits and FC



exhibited a larger deficit of grapheme-phoneme association, while patients with lower FC of the CON showed a larger verbal executive deficit. By contrast, the FC-behavior partial correlations between the GRA-PHO deficit and CON FC (bar 2) and between the vEXE deficit and left LN FC (bar 3) were not significant. Of note, the Steiger z -transform test revealed that the magnitude of the partial correlation coefficient encompassing the GRA-PHO deficit was significantly greater for left LN FC than for CON FC (bar 1 vs bar 2) (2-tailed Steiger z test, $z = 3.39$, $p = 0.0007$, corrected for FDR at $\delta = 0.05$). By contrast, the magnitude of the partial correlation coefficient encompassing the vEXE deficit was significantly larger for CON FC than for left LN FC (bar 4 vs bar 3) (2-tailed Steiger z test, $z = 4.21$, $p = 0.00001$, corrected for FDR at $\delta = 0.05$).

These analyses revealed a double dissociation connecting deficits of grapheme-phoneme knowledge selectively and preferentially to the FC of the LN within the left hemisphere. By contrast, deficits of executive functions were related to the reduction of the FC of the CON.

We then investigated whether the FC-behavior dissociation was driven by the total amount of structural damage to the LN and CON. To this aim, we repeated the main FC-behavior partial correlation analysis but we also regressed out the number of voxels lesioned within the 2 networks. Once again, we detected 2 significant FC-behavior partial correlations linking the deficit of grapheme-phoneme knowledge to left LN FC ($r = -0.43$, $p = 0.019$) and the verbal executive deficit to CON FC ($r = -0.46$, $p = 0.01$). Of note, the Steiger z -transform test revealed that the magnitude of the partial correlation coefficient involving the GRA-PHO deficit was significantly larger for left LN FC than for CON FC (2-tailed Steiger z test, $z = 3.02$, $p = 0.0025$, corrected for FDR at $\delta = 0.05$). Contrariwise, the size of the partial correlation coefficient associated with the vEXE deficit was significantly

larger for CON FC as compared to left LN FC (2-tailed Steiger z test, $z = 3.75$, $p = 0.0002$, corrected for FDR at $\delta = 0.05$). Hence, the amount of structural damage to the left LN and CON does not account for the FC-behavior double dissociation.

Discussion

In the present study, we investigated the behavioral relevance of the FC of the LN and CON for different patterns of aphasic deficits after left-hemisphere damage. The results indicated that deficits of grapheme-phoneme knowledge and verbal executive functions exhibited a moderate, yet significant correlation, whereas deficits of comprehension/lexical semantics were strongly associated with both clusters of deficits. Critically, we observed a double dissociation such that deficits of phonological processing were more correlated with the FC of the LN within the left hemisphere, and deficits of verbal executive functions were more correlated with the FC of the CON. Overall, these findings indicate that after a left-hemisphere lesion, the relevance of resting synchronization in different networks is associated with the degree of impairment of distinctive language components (e.g., phonology and verbal executive).

The behavioral results indicated a cluster of deficits of comprehension/lexical semantics, encompassing a variety of impairments such as semantic, orthographic, and syntactic processing. This cluster strongly recapitulates (6 of 9 tests) the single language factor observed in the whole cohort of patients (i.e., patients with right- and left-hemisphere damage with/without aphasic deficits) of our previous work.¹⁷ Of interest, beside this cluster we observed 2 distinct, yet modestly correlated, clusters of deficits of phonological (grapheme-phoneme knowledge) and verbal executive processing. This finding suggests that when analyses are applied

to a selected cohort of stroke patients with language deficits rather than to the entire stroke population, there is an increase of behavioral specificity within the language domain. Overall, the coexistence of a comprehension/lexical semantics, phonology, and verbal executive clusters partially mirrors the findings recently reported in a lesion-mapping study² in which language deficits were captured in 3 behavioral factors corresponding to deficits of semantics, phonology, and executive/cognition, respectively. Therefore, recent work suggests that aphasia can be conceptualized as an overall deficit of language function, with varying degrees of phonological, semantic, and executive/cognitive impairments. The relationship of the classic language syndromes to profiles of these deficits is an important issue for future work in larger samples of patients.

We reported an FC-behavior double dissociation such that phonological (grapheme-to-phoneme association) deficits were selectively linked to FC within the left LN (figure 4), whereas verbal executive deficits were preferentially associated with the FC of the CON (figure 4).

The behaviorally relevant FC involving the LN indicates that patients with poor performance in Nonword Reading exhibited decreased FC within and between the posterior (superior temporal gyrus) and anterior (inferior frontal gyrus) portions of the left LN. This pattern probably reflects the impairment of the “indirect” or “sublexical” route of reading^{31,32} devoted to the transformation of the words into their auditory counterparts based on grapheme-to-phoneme correspondences.

Neuroimaging studies in healthy individuals have indicated that grapheme-to-phoneme processing is mediated by the superior temporal gyrus and inferior frontal gyrus in the left hemisphere,^{33,34} both of which are included in the current LN. This interpretation is also supported by clinical observations of phonological deficits of repetition³⁵ and naming errors¹ after damage of the arcuate and superior longitudinal fascicles, which connect the frontal and temporal components of the present LN.³⁶ Finally, converging evidence from task-based fMRI studies in healthy individuals indicates the presence of a phonological network in frontal and temporal areas⁹ (see review in Ref. 10) that is comparable to the nodes belonging to the present LN.

The second pattern of behaviorally relevant FC indicates that deficits of executive-cognitive functions, as indexed by poor performance in Category Fluency and Complex Ideational Material, were preferentially related to a reduction of FC in the CON. This finding is in accordance with the putative function of that network in exerting top-down control of behavior by maintaining task-relevant information during task performance in a variety of cognitive domains¹³ (i.e., not only language). Albeit, Category Fluency and Complex Ideational Material assess different linguistic aspects, i.e., verbal semantic fluency and auditory comprehension, respectively, performing

well in these tests requires several executive operations supported by the CON. During Category Fluency, patients have to access their lexicon to retrieve words from the criterion category and be focused on the task for 1 minute to avoid repetition and intrusions (i.e., words not belonging to the specified category). These operations, requiring (sustained) attention, constant monitoring of working memory, and suppression of irrelevant information may be assisted by the CON, which is involved in the maintenance of task-sets²⁹ and/or alertness and arousal.¹⁴ Accordingly, a reduction of interhemispheric FC, possibly reflecting a loss in communication and coordination of the activity among anterior insulae and thalami, might be related to poor performance in the Category Fluency test. During the Complex Ideational Material test, patients are required to read short stories and then answer yes/no questions that increase in difficulty as the test proceeds. Performing this task demands several executive processes such as attention, concentration, short-term memory, and abstract reasoning,³⁰ which again may involve the CON. Another, not-exclusive possibility is that low scores on the Complex Ideational Material reflect poor cognitive effort,³⁷ which has been associated with pathological upregulation of CON regions during difficult language tasks in aphasic patients.⁷ This maladaptive recruitment of the CON during task performance would be reflected in an abnormal reduction of resting-state FC. Overall, the pattern of behaviorally relevant FC of control networks for executive deficits is consistent with an emerging account of aphasia in which domain-general networks have a central role in language after aphasic stroke.^{38,39}

Despite the large body of work on intrinsic brain activity, its significance is still under investigation. A dominant hypothesis is that ongoing brain activity as captured by resting-state FC might reflect the history of coactivated areas working in concert.^{15,40} This interpretation is based on the strong correspondence between the topography of task-evoked and intrinsic⁴¹ activity as well as on the observation that resting-state FC can be modified by learning in a behaviorally relevant manner.⁴² At the same time, several lines of evidence indicate that intrinsic activity constrains both task-evoked activity⁴³ and behavior.⁴⁴ These findings suggest a circular interplay in which previous experience and related brain coactivations shape spontaneous activity at rest, which in turn biases task-evoked activity and behavior during task performance. In this framework, a possible mechanistic interpretation of the association between behavioral impairments and off-line resting-state FC could be a “reset” of this circle. Stroke onset would represent a novel “time zero” as the anatomical damage would interrupt the normal interaction between intrinsic, task-driven activity and behavior. A focal lesion would affect the patterns of coherent intrinsic activity that normally constrains the coordinated brain activations required to perform a given task/test. Altered spontaneous activity would abnormally be reflected in task-evoked activity leading to distorted interregional interactions and poor behavioral performance. This interpretation is consistent with several task-

based fMRI studies in stroke groups indicating that during on-line performance, new brain areas are engaged⁴⁵ while those usually recruited are abnormally activated.⁴⁶ As a prediction, spontaneous recovery and rehabilitation treatment would reshape task-evoked brain activity during task performance over time (i.e., history of coactivations) leading to a restoration of coherent intrinsic activity as indexed by resting-state FC. Indeed, recent studies indicate that behavioral recovery in language⁴⁷ and attention²⁰ domains is associated with a normalization of resting-state FC. However, future studies that combine task-based and resting-state fMRI paradigms at acute and chronic stage after stroke onset are needed to directly test the “reset” hypothesis.

The current results indicate a certain degree of behavioral specificity of resting-state FC after a left-hemisphere stroke. These findings complement those observed in our previous report showing that after a right-hemisphere lesion, attention and motor deficits are selectively related to the interhemispheric FC of the corresponding networks, the dorsal attention and motor network, respectively. Similarly, previous work in healthy individuals indicates that differences in the strength of FC within a task-specific network may account for behavioral variability in the corresponding cognitive domain.⁴⁴

Limitations

The patients enrolled in the present study were not recruited on the basis of lesion location, hence the final cohort exhibited a heterogeneous lesion distribution. Further studies investigating patients with similar lesion distributions might be useful to enhance our understanding of the associations among brain damage, FC, and aphasia. Albeit, language was assessed with a detailed battery of tests, some subcomponents (e.g., phonology) may require a deeper evaluation, for instance using nonword repetition. Finally, a recent task-based fMRI study showed that the FC differential activity between the default mode network and frontotemporoparietal networks was related to speech performance in aphasic patients.⁴⁸ Hence, future studies need to investigate the relationship between aphasic deficits and FC of the default mode network with other networks.

Author contributions

A.B., G.L.S., and M.C.: designed and conceptualized the study, drafted the manuscript for intellectual content. A.B. and N.V.M.: major role in the acquisition analysis of the data.

Study funding

This work was supported by grant “Giovani Ricercatori–Ricerca Finalizzata 2013” code GR-2013-02358806 from the Ministry of Health Italy, Grant Fellowship 2016, Fondazione Umberto Veronesi, grant from the National Institute of Neurological Disorders and Stroke RO1 NS095741-01, and funds from the Rehabilitation Institute of St. Louis.

Disclosure

The authors report no disclosures relevant to the manuscript. Go to Neurology.org/N for full disclosures.

Publication history

Received by *Neurology* May 7, 2018. Accepted in final form September 11, 2018.

References

1. Schwartz MF, Faseyitan O, Kim J, Coslett HB. The dorsal stream contribution to phonological retrieval in object naming. *Brain* 2012;135:3799–3814.
2. Butler RA, Lambon Ralph MA, Woollams AM. Capturing multidimensionality in stroke aphasia: mapping principal behavioural components to neural structures. *Brain* 2014;137:3248–3266.
3. Jefferies E, Lambon Ralph MA. Semantic impairment in stroke aphasia versus semantic dementia: a case-series comparison. *Brain* 2006;129:2132–2147.
4. Bates E, Wilson SM, Saygin AP, et al. Voxel-based lesion-symptom mapping. *Nat Neurosci* 2003;6:448–450.
5. Dronkers NF. A new brain region for coordinating speech articulation. *Nature* 1996;384:159–161.
6. Saur D, Lange R, Baumgaertner A, et al. Dynamics of language reorganization after stroke. *Brain* 2006;129:1371–1384.
7. Brownsett SL, Warren JE, Geranmayeh F, Woodhead Z, Leech R, Wise RJ. Cognitive control and its impact on recovery from aphasic stroke. *Brain* 2014;137:242–254.
8. Boukhrina O, Barrett AM, Alexander EJ, Yao B, Graves WW. Neurally dissociable cognitive components of reading deficits in subacute stroke. *Front Hum Neurosci* 2015;9:298.
9. Heim S, Friederici AD. Phonological processing in language production: time course of brain activity. *Neuroreport* 2003;14:2031–2033.
10. Vigneau M, Beaucousin V, Herve PY, et al. Meta-analyzing left hemisphere language areas: phonology, semantics, and sentence processing. *Neuroimage* 2006;30:1414–1432.
11. Baldo JV, Schwartz S, Wilkins D, Dronkers NF. Role of frontal versus temporal cortex in verbal fluency as revealed by voxel-based lesion symptom mapping. *J Int Neuropsychol Soc* 2006;12:896–900.
12. Wagner S, Sebastian A, Lieb K, Tuscher O, Tadic A. A coordinate-based ALE functional MRI meta-analysis of brain activation during verbal fluency tasks in healthy control subjects. *BMC Neurosci* 2014;15:19.
13. Dosenbach NU, Visscher KM, Palmer ED, et al. A core system for the implementation of task sets. *Neuron* 2006;50:799–812.
14. Sadaghiani S, D’Esposito M. Functional characterization of the cingulo-opercular network in the maintenance of tonic alertness. *Cereb Cortex* 2015;25:2763–2773.
15. Fox MD, Raichle ME. Spontaneous fluctuations in brain activity observed with functional magnetic resonance imaging. *Nat Rev Neurosci* 2007;8:700–711.
16. Siegel JS, Ramsey LE, Snyder AZ, et al. Disruptions of network connectivity predict impairment in multiple behavioral domains after stroke. *Proc Natl Acad Sci USA* 2016;113:E4367–E4376.
17. Corbetta M, Ramsey L, Callejas A, et al. Common behavioral clusters and subcortical anatomy in stroke. *Neuron* 2015;85:927–941.
18. Baldassarre A, Ramsey L, Hacker CL, et al. Large-scale changes in network interactions as a physiological signature of spatial neglect. *Brain* 2014;137:3267–3283.
19. Baldassarre A, Ramsey L, Rengachary J, et al. Dissociated functional connectivity profiles for motor and attention deficits in acute right-hemisphere stroke. *Brain* 2016;139:2024–2038.
20. Ramsey LE, Siegel JS, Baldassarre A, et al. Normalization of network connectivity in hemispatial neglect recovery. *Ann Neurol* 2016;80:127–141.
21. Shulman GL, Pope DL, Astafiev SV, McAvoy MP, Snyder AZ, Corbetta M. Right hemisphere dominance during spatial selective attention and target detection occurs outside the dorsal frontoparietal network. *J Neurosci* 2010;30:3640–3651.
22. Fox MD, Zhang D, Snyder AZ, Raichle ME. The global signal and observed anti-correlated resting state brain networks. *J Neurophysiol* 2009;101:3270–3283.
23. Power JD, Barnes KA, Snyder AZ, Schlaggar BL, Petersen SE. Spurious but systematic correlations in functional connectivity MRI networks arise from subject motion. *Neuroimage* 2012;59:2142–2154.
24. Siegel JS, Snyder AZ, Ramsey L, Shulman GL, Corbetta M. The effects of hemodynamic lag on functional connectivity and behavior after stroke. *J Cereb Blood Flow Metab* 2015;36:2162–2176.
25. Hacker CD, Laumann TO, Szrama NP, et al. Resting-state network estimation in individual subjects. *Neuroimage* 2013;82:616–633.
26. Steiger JH. Testing pattern hypotheses on correlation matrices: alternative statistics and some empirical results. *Multivariate Behav Res* 1980;15:335–352.
27. Diedenhofen B, Musch J. cocor: a comprehensive solution for the statistical comparison of correlations. *PLoS One* 2015;10:e0121945.
28. Benjamini Y, Hochberg Y. Controlling the false discovery rate: a practical and powerful approach to multiple testing. *J R Stat Soc Ser B* 1995;57:289–300.
29. Shao Z, Janse E, Visser K, Meyer AS. What do verbal fluency tasks measure? Predictors of verbal fluency performance in older adults. *Front Psychol* 2014;5:772.
30. Riegel B, Bennett JA, Davis A, et al. Cognitive impairment in heart failure: issues of measurement and etiology. *Am J Crit Care* 2002;11:520–528.

31. Paap KR, Noel RW. Dual-route models of print to sound: still a good horse race. *Psychol Res* 1991;53:13–24.
32. Coltheart M, Curtis B, Atkins P, Haller M. Models of reading aloud: dual-route and parallel-distributed-processing approaches. *Psychol Rev* 1993;100:589–608.
33. Jobard G, Crivello F, Tzourio-Mazoyer N. Evaluation of the dual route theory of reading: a meta-analysis of 35 neuroimaging studies. *Neuroimage* 2003;20:693–712.
34. Joubert S, Beauregard M, Walter N, et al. Neural correlates of lexical and sublexical processes in reading. *Brain Lang* 2004;89:9–20.
35. Kummerer D, Hartwigsen G, Kellmeyer P, et al. Damage to ventral and dorsal language pathways in acute aphasia. *Brain* 2013;136:619–629.
36. Saur D, Kreher BW, Schnell S, et al. Ventral and dorsal pathways for language. *Proc Natl Acad Sci USA* 2008;105:18035–18040.
37. Erdodi L, Roth R. Low scores on BDAE Complex Ideational Material are associated with invalid performance in adults without aphasia. *Appl Neuropsychol Adult* 2016;24:264–274.
38. Fedorenko E. The role of domain-general cognitive control in language comprehension. *Front Psychol* 2014;5:335.
39. Geranmayeh F, Brownssett SL, Wise RJ. Task-induced brain activity in aphasic stroke patients: what is driving recovery? *Brain* 2014;137:2632–2648.
40. Deco G, Corbetta M. The dynamical balance of the brain at rest. *Neuroscientist* 2011;17:107–123.
41. Cole MW, Bassett DS, Power JD, Braver TS, Petersen SE. Intrinsic and task-evoked network architectures of the human brain. *Neuron* 2014;83:238–251.
42. Lewis CM, Baldassarre A, Committeri G, Romani GL, Corbetta M. Learning sculpts the spontaneous activity of the resting human brain. *Proc Natl Acad Sci USA* 2009;106:17558–17563.
43. Cole MW, Ito T, Bassett DS, Schultz DH. Activity flow over resting-state networks shapes cognitive task activations. *Nat Neurosci* 2016;19:1718–1726.
44. Baldassarre A, Lewis CM, Committeri G, Snyder AZ, Romani GL, Corbetta M. Individual variability in functional connectivity predicts performance of a perceptual task. *Proc Natl Acad Sci USA* 2012;109:3516–3521.
45. Turkeltaub PE, Messing S, Norise C, Hamilton RH. Are networks for residual language function and recovery consistent across aphasic patients? *Neurology* 2011;76:1726–1734.
46. Corbetta M, Kincade MJ, Lewis C, Snyder AZ, Sapir A. Neural basis and recovery of spatial attention deficits in spatial neglect. *Nat Neurosci* 2005;8:1603–1610.
47. Marangolo P, Fiori V, Sabatini U, et al. Bilateral transcranial direct current stimulation language treatment enhances functional connectivity in the left hemisphere: preliminary data from aphasia. *J Cogn Neurosci* 2016;28:724–738.
48. Geranmayeh F, Leech R, Wise RJ. Network dysfunction predicts speech production after left hemisphere stroke. *Neurology* 2016;86:1296–1305.